

Morphological Control of Helical Solid Bilayers in High-Axial-Ratio Nanostructures Through Binary Self-Assembly

George John,^{*,[a]} Jong Hwa Jung,^[a] Hiroyuki Minamikawa,^[b] Kaname Yoshida,^[b] and Toshimi Shimizu^{*,[a, b]}

Abstract: Mixed molecular species of cardanyl glucoside derived from renewable resources provide nanotubes upon self-assembly in water, while the saturated homologue generated a twisted fibrous morphology. The cardanyl glucoside mixture was fractionated into four individual components in order to study their contribution to the nanotube formation. The rational control of self-assembled helical morphologies was achieved by binary self-assembling of the saturated and monoene derivatives. This method can generate a diversity of self-assembled high-axial-ratio nanostructures (HARNs), ranging from twisted ribbons and helical ribbons to nanotubes.

Keywords: glycolipids • helical solid bilayers • morphological control • nanostructures • self-assembly

Introduction

Currently, there is tremendous interest in high-axial-ratio nanostructures (HARNs) formed by the hierarchical self-assembly of amphiphilic molecules into helical ribbons and nanotubes.^[1] The need for improved miniaturisation and device performance in the microchip and microelectronics industry has inspired many investigations into supramolecular chemistry. It is conceivable that the “bottom-up”^[2] HARN-fabrication approaches based on supramolecular chemistry will provide a solution to the anticipated size limitations of “top-down” approaches, such as photolithography,^[3] thereby providing the means to fabricate ultra-small electronic components. However, the discovery of such materials remains a time consuming and rather unpredictable trial and error process. Hence there is a need for a more efficient and systematic approach for the generation of novel HARN libraries by using existing lead molecules with appropriate mixing and self-assembly methods.

Combinatorial synthesis and screening of very large numbers of organic compounds has been widely applied in the pharmaceutical industry for drug discovery.^[4] Recently, combinatorial arrays of inorganic materials with known or potential applications have been synthesised and screened.^[5] Also there are efforts to design catalysts,^[6] functional polymers,^[7] synthetic molecular receptors^[8] and other new materials by using the combinatorial approach.^[9] Despite the utility of combinatorial chemistry for the efficient investigation of systems that involve numerous interrelated variables, the application of such strategies to controlling the HARN structures remains underexplored. The discovery and development of new compositions and compounds for tuned morphologies is of great importance for the development of new molecular architectures, like lipid nanotubes, twisted and helical ribbons, which may have potential applications in health care, proteomics and templates for sub-microchip, sub- μ -TAS applications. We have reported so far the preparation of various HARNs, including helical fibres and microtubes, through molecular self-assembly.^[1h, 10] Recently we found the facile synthesis of lipid nanotubes through the self-assembly of glycolipids^[11] derived from cardanol^[12] (a renewable resource and a mixture of four components). The morphology of tubules must be rationally optimised for each application. Therefore it is important to understand the role the various constituent molecules play in the formation of these structures, and thus we successfully fractionated each component of the mixture. Here we describe a simple combinatorial approach for synthesising and characterising new helical HARN structures by mixing compounds **1** and **2** for optimal properties. Though there have been efforts to control the

[a] Dr. G. John, Prof. T. Shimizu, Dr. J. H. Jung
CREST, Japan Science and Technology Corporation (JST)
NARC, AIST, Tsukuba Central 4, 1-1-1 Higashi
Tsukuba, Ibaraki 305-8562 (Japan)
Fax: (+81)298-61-2659
E-mail: george-john@aist.go.jp
shnz-shimizu@aist.go.jp

[b] Prof. T. Shimizu, Dr. H. Minamikawa, Dr. K. Yoshida
Nanoarchitectonics Research Center (NARC)
National Institute of Advanced Industrial Science and Technology
Tsukuba Central 5, 1-1-1 Higashi
Tsukuba, Ibaraki 305-8565 (Japan)
Fax: (+81)298-61-4545

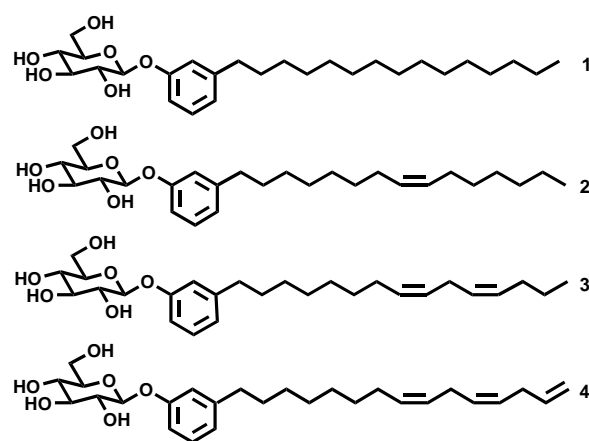
morphology of self-assembled microstructures^[13] by concentration change and the solvent polarity of the system,^[14] the approach of varying the composition of two lead molecules of definite morphology to form a desired structure is new.

Our application of bottom-up construction of HARN structures by hierarchical self-assembly of small molecules in water, exemplified by the cardanyl glucoside components discussed here, involves the following steps: miscible mixing and self-assembly of the compounds, screening of the self-assembled structures by microscopic and other methods. Initially an 11-membered library was derived from the compounds **1** and **2** by mixing and further self-assembly in water. Once a suitable composition has been identified that demonstrates the desired activity (morphology), efforts can then turn towards optimising the conditions and system to yield the desired selectivity. This two-tiered development strategy can offer distinct advantages in the discovery and identification of new compositions for the generation of controlled helical HARN structures of solid bilayers including tubular structures.

Results and Discussion

The gram-scale separation of cardanyl glucoside into its individual components was achieved with medium-pressure ODS (octadecylsilyl 50 μm) column chromatography. The triene fraction separated first, and subsequently diene, monoene and saturated components were eluted by using methanol/10% aqueous acetic acid. Each fractionated component was tested by using NMR spectroscopy and other analytical methods for its purity and structure determination. The thermal behaviour of the diene and triene in the fully hydrated form display a gel-to-liquid crystalline phase transition at 17.0 °C and –25.0 °C, respectively; this suggests that the diene and triene glucosides are in a fluid state at room temperature. Therefore, evidently the self-assembly of those structures into solid fibrous materials at room temperature is ruled out. Thus we assume that the saturated and monoene components play the major role in the nanotube formation mechanism of cardanyl glucoside. We identified them as lead molecules **1** and **2** for further mixing and binary self-assembly processes for desired compositions (Scheme 1). The compounds **1** and **2** were mixed in many proportions ranging from 0 to 100% as depicted in (Figure 1). Self-assembly of the pure components as well as the mixture of glycolipids was carried out in water at boiling temperature and cooled to room temperature under ambient conditions.

Morphology analysis: The morphological information on the self-assembled helical HARNs was obtained by field-emission scanning electron microscopy without the need for metal coating. The self-assembled structures of both pure and mixed lipids were used for the microscopy. The pure saturated analogue **1** showed a twisted fibrous morphology in FE-SEM with an unstained sample (Figure 2a). In contrast, on self-assembly in water, the pure monoene component **1** resulted in nanotube formation including partly tightly coiled nanofibres. The tightly coiled fibres might be the precursor for nanotube



Scheme 1. Fractionated components from cardanyl glucoside.

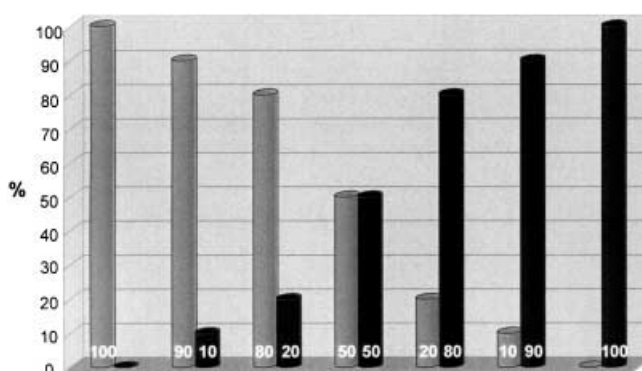


Figure 1. Library of compositions by mixing and binary self-assembly of lead molecules **1** (saturated, left) and **2** (monoene, right).

formation as in Figure 2g. Self-assembly of mixed lipids generated a library of nine diverse sets of compositions and was analysed by FE-SEM. Typically the 90:10 (saturated/monoene) mixture self-assembled to form twisted ribbons in water, as shown in Figure 2b; this might be expected for the 10% doping of the monoene component. The 80:20 compositions also showed twisted-ribbon morphology on FE-SEM analysis (Figure 2c). No remarkable effect on the twisted morphology was observed by doping of the monoene component by up to 30–40%. On the other hand, an equimolar (50:50) composition gave a loosely coiled ribbon morphology, in between the twisted and tight helical coil (Figure 2d). On increasing the monoene content in these libraries, the helical pitch decreases to give tubular morphologies characterised by a definite hollow cylinder with helical markings (Figure 2e, f) in comparison with the nanotubes obtained from pure monoene (Figure 2g) and from cardanyl glucoside (Figure 2h), which had smooth surfaces. A schematic illustration of the various helical morphologies described above is depicted in Figure 3 for comparison and clarity. The samples were aged under ambient conditions for 150 days, and the morphology changes were studied by energy-filtering transmission electron microscopy (EF-TEM). The TEM micrographs showed without any doubt that the morphologies remain intact after the ageing of the

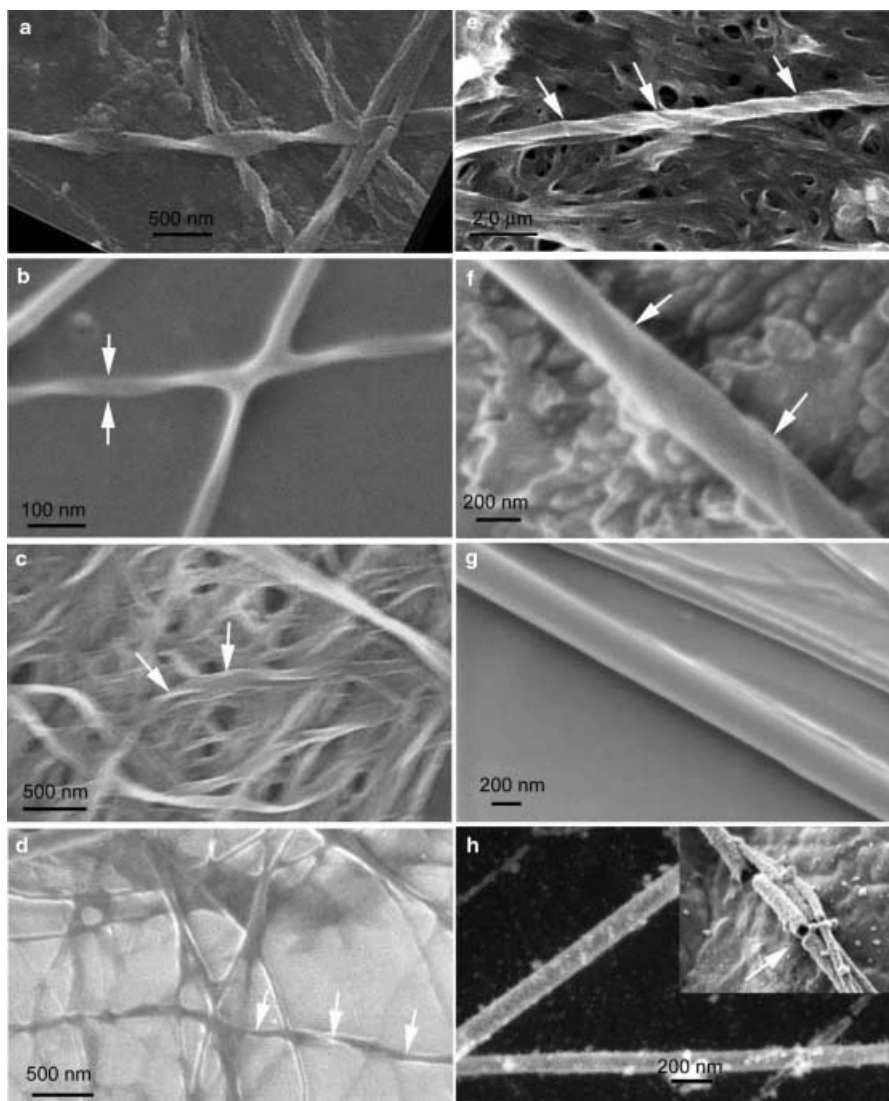


Figure 2. FE-SEM images of self-assembled HARNs after 2 days' incubation (saturated/monoene): a) 100:0, b) 90:10,^[a] c) 80:20,^[a] d) 50:50,^[a] e) 20:80,^[b] f) 10:90,^[c] g) 0:100 and h) cardanyl glucoside mixtures, as a reference. [a] the white arrows indicate twisted helical morphology, [b] the white arrows show the tightly coiled helical ribbons and [c] helical markings on the nanotubes.

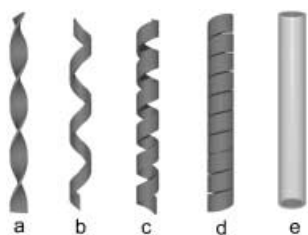


Figure 3. Schematic representations of the morphologies of helical solid bilayers in HARNs: a) twisted ribbon, b) loosely coiled ribbon, c) tightly coiled ribbon, d) tubule with helical marking, e) tubule without helical marking.

samples (Figure 4) and are very similar to the morphologies obtained by FE-SEM immediately after the preparation of the sample (within 2 days). It seems to be significant that one could regulate the morphology of HARNs by appropriate mixing and self-assembly of existing lead molecules.

CD studies: The microscopic chiral packing features of molecules can be studied through circular dichroism (CD) spectroscopy. CD is often used to characterise the chiral optical properties of molecules in solution. However, when molecules form chiral aggregates, nonchiral molecular absorption peaks can become chirally active, with differential absorption of left- and right-handed circularly polarised light. Hence, CD peaks can indicate a chiral structure of the aggregates rather than of the individual molecules. The circular dichroism of the saturated and the monoene lipid helical ribbons has been studied in water. Figure 5 shows the CD spectra of the monoene fraction in comparison with the saturated compound in a self-assembled state at 25 °C. The experiments showed that the nanotubes/coiled helical ribbons have a relatively high CD signal, depending on the concentration of the assemblies; the CD intensity is at least 200 times higher than that of the saturated analogue self-assembling into twisted fibres. When the solution is heated to a temperature above the corresponding gel-to-liquid-crystal phase transition, the CD signal gradually drops to zero as the tubules transform into spherical vesicles at each

phase-transition temperature (Figure 5B). The disappearance of the CD peaks at temperatures above the phase transition demonstrates that the recorded CD signal is the result of supramolecular chirality.^[15] The UV spectrum of monomer self-assembly in water displays a typical absorption at 196 nm (Figure 5A), which might be due to the stacked π electrons in a helical environment due to aromatic stacking. Thus the CD results show that the coiled or tubular structures are based on *nonparallel* chiral packing due to the “kink” structure expressed by the *cis* double bond on the monoene, whereas the saturated analogue self-assembled to twisted fibres formed by *parallel* chiral packing, as discussed in the literature.^[14a, 16]

DSC analysis of self-assemblies: Self-assembled fibre was isolated from the aqueous dispersion with a centrifuge at 3500 rpm, and the settled sample was isolated and used for the differential scanning calorimetry (DSC) measurements. The phase transition of the saturated and monoene components of

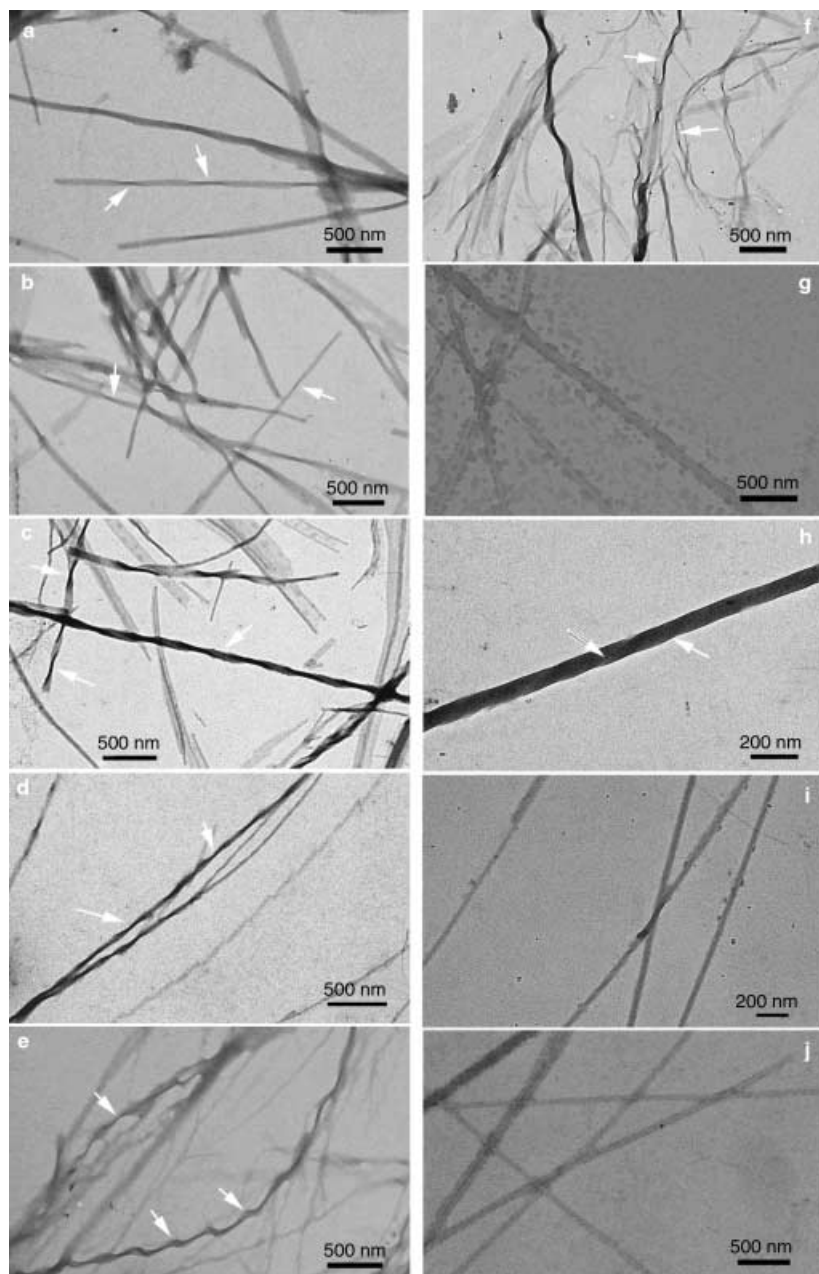


Figure 4. FE-TEM images of self-assembled HARNs after 150 days' incubation (saturated/monoene): a) 100:0,^[a] b) 90:10,^[a] c) 80:20,^[a] d) 60:40,^[a] e) 50:50,^[b] f) 40:60,^[a] g) 30:70, h) 20:80,^[c] i) 10:90 and j) 0:100. [a] white arrows indicate twisted helical morphology, [b] white arrows show the loosely coiled ribbon, [c] tightly coiled ribbon.

the cardanyl glucoside mixture have not previously been studied by DSC. The saturated component showed a phase transition at 77.8 °C, while on introduction of a single *cis* double bond in the aliphatic chain the phase transition decreases to 38.5 °C (Table 1). High-sensitivity DSC is applied to determine the miscibility of the lipids **1** and **2** in the fully hydrated state. The gel-to-liquid-crystalline phase-transition data for the pure and mixed lipids are shown in Figure 6. Ideally mixed binary systems should show a single peak between the T_{ms} of the two pure components. As can be seen, the mixed systems exhibit single transitions in the range of monoene fractions up to 30% in the mixture of **1** and **2** in between the pure lipids; this implies an ideal mixing pattern. Even though the concentration conditions employed are

much higher (~2000 times) relative to that for self-assembly, some phase separation seems to occur for the mixed system with a concentration range of 50:50 wt% as evident from multiple melting profiles for the compositions of monoene/saturated mixtures (60:40, 50:50 and 40:60). The DSC data clearly demonstrate that the self-assembled HARNs are in the solid state at room temperature, irrespective of their morphological difference. The phase-transition temperature increases with the increase in concentration of the saturated component as plotted in (Figure 6).

X-ray diffraction studies: The DSC studies gave information on the phase transitions occurring in the bilayers and the self-assembled structures. To gain insight into the molecular orientation and packing profile within the each HARN, we performed small-angle X-ray scattering studies by using the isolated self-assembled fibres as both wet and dried samples. The values indicate that, upon mixing the saturated analogue and monoene component, the molecular arrangement seems to be rather similar to pure components that take on interdigitated bilayer structures.^[11] It should be noted that the molecular orientation and packing within the fibres are dif-

ferent in both compounds, depending on whether the long hydrocarbon chain is saturated or unsaturated. The monoene **2**-rich binary mixtures gave a d spacing of 3.9 nm, in comparison with the shorter ($d=3.1$ nm) spacing of the saturated glycolipid **1**; this suggests an interdigitated morphology, since the extended molecular lengths of **1** and **2** can be evaluated to about 3 nm. Moreover, the saturated glycolipid shows higher ordering in the aliphatic region, possibly due to hydrocarbon crystallisation. Furthermore, this suggests that the present glucosides are easily miscible with the second component up to 30% wt% without disturbing the molecular packing of the host molecule (major component). Once the concentration of the minor component reaches 40% wt, the composite tends to phase separate, as indicated by a splitting

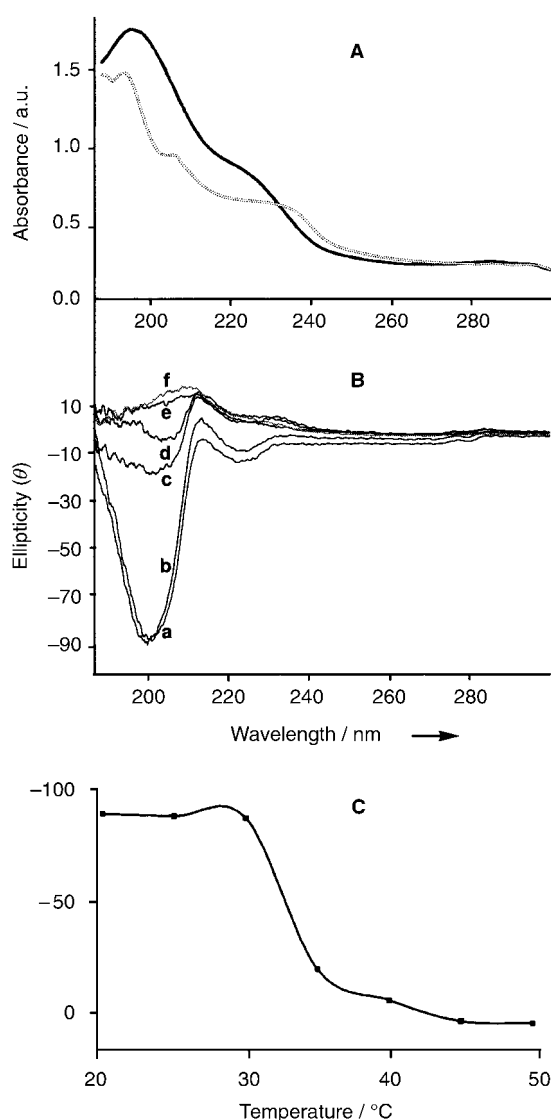


Figure 5. A) UV absorption spectra of self-assembled aggregates in water: saturated **1** (····) and monoene **2** (—) at 25 °C. $\lambda_{\text{max}} = 196$ nm (major absorption). Concentration of saturated **1** = 2.3×10^{-5} and of monoene **2** = 2.3×10^{-5} molL⁻¹ (All concentrations mentioned are for monomer species). B) Temperature-dependant CD spectra of **2** helical morphologies in water (a: 25, b: 30, c: 35, d: 40, e: 45 °C) and saturated **1** (f: 25 °C, dotted line). C) The intensity of the CD peaks at 196–200 nm decreased as a function of temperature. Concentration of saturated **1** = 2.3×10^{-5} and monoene **2** = 2.3×10^{-5} molL⁻¹ (All concentrations mentioned are for monomer species).

Table 1. HARN libraries with different morphologies and their physical data.

Composition 2/1	DSC data $T_{g,i}$ [°C]	XRD data ^[c] d [nm]	FE-SEM morphology
100:0	38.5 ^[a]	3.96	tubule(no helical marking) ^[d]
90:10	40.4 ^[b]	3.96	tubule (helical marking)
80:20	42.5 ^[b]	3.96	loosely coiled ribbon
50:50	51.0, 47.8 ^[b]	3.90, 3.22	twisted ribbon (low pitch)
20:80	74.3 ^[b]	3.10	twisted ribbon
10:90	75.4 ^[b]	3.14	twisted ribbon
0:100	77.8 ^[a]	3.14	twisted ribbon

[a] Measured for self-assembled fibres. [b] Measured for binary mixture. [c] Measured for self-assembled structures. [d] Partly include tightly coiled ribbons.

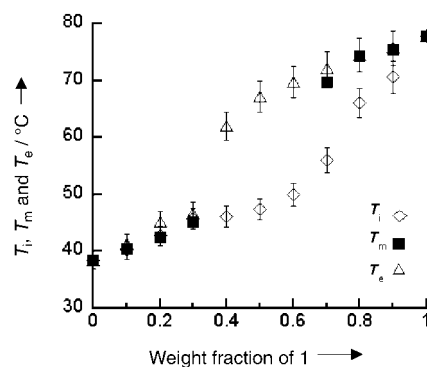


Figure 6. Composition-dependent phase-transition behaviour of the self-assembled HARNs. T_i and T_e are corrected onset and completion temperatures. Error bars are standard errors. If two values lie within the error bars, the difference between these values is statistically insignificant.

of the XRD peak in the long-range order; this also supports the DSC data. The values of molecular periodicity are in the range 3.1–3.96 nm, measured for pure saturated components **1** and **2**, though the compositional variation shows clear morphological changes in the FE-SEM, TEM analysis and DSC values.

Conclusion

The tuning of HARN structures of solid bilayers was achieved by using two lead molecules with small but definite structural variations. The present binary self-assembly in water, which yields intermediate morphologies can lead to the preparation of extensive HARN libraries as represented in Figure 1. This simple combinatorial design of HARNs will accelerate progress in preparing and evaluating novel nanostructured materials with existing amphiphilic compounds. Although studies on morphological regulations by changing concentration and solvent systems have been conducted in the past, the lack of common structural features among lead compounds made it difficult to correlate the structure and molecular morphology upon self-assembly. The further study of combinatorial design of HARN structures will facilitate the identification of new morphologies that are optimally matched to the requirements of a specific nanostructure application for miniaturisation.

Experimental Section

Instrumental methods: Differential scanning calorimetry (DSC) was performed on a Seiko DSC6100 high-sensitivity differential scanning calorimeter equipped with a nitrogen gas cooling unit. The lipid suspension was hermetically sealed in a silver pan and measured against a pan containing alumina as the reference. With pure lipids and mixtures, concentrations of 1–2 mgmL⁻¹ were used. The thermograms were recorded at a heating rate of 1 °Cmin⁻¹. X-ray powder diffraction (XRD) patterns were measured by using a Rigaku diffractometer (Type 4037) with graded d -space elliptical side-by-side multiplayer optics, monochromated Cu_{K α} radiation (40 kV, 30 mA), and imaging plate (R axis IV). The fibrous sample was transferred to a quartz capillary tube, and excess water was removed by using a syringe. The capillary was sealed, and the XRD was

measured. The typical exposure time was 5 min for self-assembled structures with 150 mm camera length. Field-emission scanning electron microscopy (FE-SEM) studies were carried out on a Carl Zeiss LEO GEMINI 1550 (accelerating voltage: 0.4–0.7 kV, working distance: 3–4 mm). The SEM samples were prepared by transferring 15 μL of the lipid suspension onto a 400 mesh carbon-coated Formvar copper grid. Excess water was removed by touching the edge of the grid with filter paper. The samples were allowed to dry in air prior to imaging. Circular dichroism (CD) studies were performed on a JASCO-720 spectropolarimeter operating between 175 and 700 nm. The samples were placed in water-jacketed quartz cells with path lengths of 0.1 to 0.5 mm. Temperature control was provided by a water circulator, which provided a thermal stability of about 0.2 °C. The spectrometer was calibrated with ammonium-D-camphorsulfonate ($[\theta]_{291} = 7910^\circ \text{cm}^2 \text{dmol}^{-1}$) and D-pantoyllactone ($[\theta]_{219} = -16140$ in water, $[\theta]_{223} = -12420$ in methanol). Cardanyl glucoside mixtures were fractionated by using a Yamazen fraction collector FR-50N coupled with a gradient mixer GR-200, variable-wavelength UV detector prep UV-10-V and a flat mini recorder. The sample was subjected to medium-pressure column chromatography on a Yamazen ODS column (100 \times 2.6 cm, *i.d.*) packed with ODS (50 μm particle size). The mobile phase used was methanol/10% aqueous acetic acid (initially 88:12, after the sample injection the gradient changed to 90:10, *v/v*) and delivered with a Yamazen Peristatic pump at 8 mL min^{-1} . The effluent was monitored by the UV detector at 254 nm. The fractions were collected and dried to constant weight under vacuum at room temperature.

Materials and general methods: Cardanyl glucoside was prepared by coupling of cardanol with D-glucose by a simple glycosylation method,^[11] and is a mixture of four components; **1**: 1-*O*-3'-*n*-(pentadecyl)phenyl- β -D-glucopyranoside (5%), **2**: 1-*O*-3'-*n*-(8'(Z)-pentadecenyl)phenyl- β -D-glucopyranoside (50%), **3**: 1-*O*-3'-*n*-(8'(Z),11'(Z)-pentadecadienyl)phenyl- β -D-glucopyranoside (16%) and **4**: 1-*O*-3'-*n*-(8'(Z),11'(Z),14'-pentadecatrienyl)phenyl- β -D-glucopyranoside (29%). Cardanol was obtainable by double vacuum distillation of cashew-nut-shell liquid (CNSL) at 3–4 mmHg and the fraction boiling between 220–235 °C was collected. The compounds for the present study, **1** and **2**, were obtained by the fractionation of the cardanyl glucoside mixture into its individual components by reverse-phase medium-pressure column chromatography. The compounds corresponding to the saturated **1**, monoene **2**, diene **3** and triene **4** components were isolated and analysed by standard methods. The fractionated amount of compound **1** was not sufficient for further detailed experimental studies, and thus we synthesised it in the laboratory by using the same procedure as for **2** described earlier.^[11]

Saturated 1: m.p. 143.6 °C; ¹H NMR (600 MHz, [D₄]CH₃OH, 25 °C, TMS): $\delta = 0.88$ (t, 3H; Me), 1.25 (m, 24H; CH₂), 1.58 (m, 2H; CH₂CH₂Ar), 2.56 (t, 2H; CH₂Ar), 3.13–3.69 (m, H2, H3, H4, H5 and H6), 4.82 (d, ²J(H,H) = 7.3 Hz, 1H; H1), 6.79 (d, 2H), 6.80–6.89 (d, 1H), 7.19–7.20 (t, 1H); ESI mass: 466; elemental analysis calcd (%) for C₂₇H₄₆O₆ (466.0): C 69.493, H 9.935; found: C 68.993, H 9.876.

Monoene 2: m.p. 132 °C; ¹H NMR (600 MHz, [D₄]CH₃OH, 25 °C, TMS): $\delta = 0.88$ (t, 3H; Me), 1.25 (m, 16H; CH₂), 1.58 (m, 2H; CH₂CH₂Ar), 2.00 (CH₂CH=CH₂, 4H), 2.56 (t, 2H; CH₂Ar), 3.13–3.69 (m, H2, H3, H4, H5 and H6), 4.82 (d, ²J = 7.3 Hz, 1H; H1), 5.3 (t, 2H; vinyl protons), 6.79 (d, 2H), 6.80–6.89 (d, 1H), 7.19–7.20 (t, 1H); ESI mass: 464; elemental analysis calcd (%) for C₂₇H₄₄O₆ (464.0): C 69.82, H 9.48; found: C 69.41, H 9.46.

Diene 3: m.p. 115 °C; ¹H NMR (600 MHz, [D₄]CH₃OH, 25 °C, TMS): $\delta = 0.88$ (t, 3H; Me), 1.25 (m, 8H; CH₂), 1.35–1.4 (m, CH₂CH₃), 1.58 (m, 2H; CH₂CH₂Ar), 2.00 (CH₂CH=CH₂), 2.56 (t, 2H; CH₂Ar), 2.78 (m, 2H, CH=CHCH₂CH=CH), 3.13–3.69 (m, H2, H3, H4, H5 and H6), 4.82 (d, ²J_{1,2} = 7.3 Hz, 1H; H1), 5.3 (m, 4H; vinyl protons), 6.79 (d, 2H), 6.80–6.89 (d, 1H), 7.19–7.20 (t, 1H); ESI mass: 462; elemental analysis calcd (%) for C₂₇H₄₂O₆ (462.0): C 70.12, H 9.09; found: C 69.943, H 8.973.

Triene 4: m.p. 96 °C; ¹H NMR (600 MHz, [D₄]CH₃OH, 25 °C, TMS): $\delta = 1.25$ (m, 8H; CH₂), 1.58 (m, 2H; CH₂CH₂Ar), 2.00 (CH₂CH=CH₂), 2.56 (m or t, 2H; CH₂Ar), 2.78 (m, 4H; CH=CHCH₂CH=CH), 3.13–3.69 (m, H2, H3, H4, H5 and H6), 4.82 (d, ²J_{1,2} = 7.3 Hz, 1H; H1), 4.9–5.05 (tt, 2H; vinyl protons), 5.3–5.45 (m, 4H; vinyl protons), 5.75–5.85 (m, 1H; vinyl protons), 6.79 (d, 2H), 6.80–6.89 (d, 1H), 7.19–7.20 (t, 1H); ESI mass: 460; elemental analysis calcd (%) for C₂₇H₄₀O₆ (460.0): C 70.43, H 8.69; found: C 69.982, H 8.72.

Self-assembly experiments: The compounds **1** and **2** were dissolved separately in methanol and quantitatively mixed in a flask for a series of compositions (0–100%), the solvent was evaporated, and the residue was dried under vacuum for 3 h. Up to 10 simultaneous self-assembly experiments on a 3 mg scale were conducted in separate flasks. Since the compounds used had almost identical structures and behaviour, the same set of experimental conditions was employed. The samples were dispersed in Milli-Q water (100 mL), gradually heated to boiling and kept for 1 h for thorough mixing and dispersing. The transparent aqueous dispersion was gradually cooled to room temperature and kept without shaking. This methodology can be used for the automated self-assembly process of HARN library preparations. After several hours, the self-assembled material appeared as a white cotton-like mass and was collected (within 24 h) for various analyses by wet and dry methods.

Miscibility studies: The miscibility of the glycolipids **1** and **2** was studied by differential scanning calorimetry (DSC). Stock solutions of both glycolipids in methanol were quantitatively mixed in a sample bottle, the solvent was removed under a stream of nitrogen, and the sample was dried overnight in vacuo. Weighed amounts (~2 mg) of the sample were transferred to a silver capsule. After addition of Milli-Q water (~20 mg), the samples were sealed and kept for 12 h to complete the hydration. DSC experiments were conducted at a heating rate of 1 °C min^{-1} for repeated heating-cooling cycles to ensure thorough mixing and complete hydration of the glycolipids.

Acknowledgements

We thank Shigeaki Tachibana of Carl Zeiss, Tokyo for assistance with the FE-SEM and Rika Iwaura for the drawings.

- [1] a) T. Kunitake, *Angew. Chem.* **1992**, *104*, 692–710; *Angew. Chem. Int. Ed. Engl.* **1992**, *31*, 709–726; b) J. M. Schnur, *Science* **1993**, *262*, 1669–1676; c) J.-H. Fuhrhop, W. Helfrich, *Chem. Rev.* **1993**, *93*, 1565–1582; d) J.-H. Fuhrhop, J. Koning, *Membranes and Molecular Assemblies: The Synkinetic Approach* (Ed.: J. F. Stoddart), The Royal Society of Chemistry, Cambridge, **1994**; e) P. Terech, R. G. Weiss, *Chem. Rev.* **1997**, *97*, 3133–3159; f) M. C. Feiters, R. J. M. Nolte in *Advances in Supramolecular Chemistry* (Ed. G. W. Gokel), JAI Press, **2000**, pp. 41–156; g) J. H. Jung, H. Kobayashi, M. Masuda, T. Shimizu, S. Shinkai, *J. Am. Chem. Soc.* **2001**, *123*, 8785–8789; h) T. Shimizu, *Macromol. Rapid. Commun.* **2002**, *23*, 311–331; i) E. Wilson-Kubalek, R. E. Brown, H. Celia, R. A. Milligan, *Proc. Natl. Acad. Sci. USA* **1998**, *95*, 8040–8045; j) Y. V. Zastavker, N. Asherie, A. Lomakin, J. Pande, J. M. Donovan, J. M. Schnur, G. B. Benedek, *Proc. Natl. Acad. Sci. USA* **1999**, *96*, 7883–7887; k) R. Oda, I. Huc, M. Schmutz, S. J. Candau, F. C. MacKintosh, *Nature* **1999**, *399*, 566–569; l) D. A. Frankel, D. F. O'Brien, *J. Am. Chem. Soc.* **1994**, *116*, 10057–10069.
- [2] G. M. Whitesides, J. P. Mathias, C. T. Seto, *Science* **1991**, *254*, 1312–1319.
- [3] Y. Xia, G. M. Whitesides, *Angew. Chem.* **1998**, *110*, 568–594; *Angew. Chem. Int. Ed.* **1998**, *37*, 550–575.
- [4] H. M. Geysen, R. H. Meloan, S. J. Barteling, *Proc. Natl. Acad. Sci. USA* **1984**, *81*, 3998–4002; b) B. A. Bunin, J. A. Ellman, *J. Am. Chem. Soc.* **1992**, *114*, 1097–1098; c) B. A. Bunin, M. J. Plunkett, J. A. Ellman, *Proc. Natl. Acad. Sci. USA* **1994**, *91*, 4708–4712.
- [5] a) X.-D. Xiang, X. Sun, G. Briceno, Y. Lou, K.-A. Wang, H. Chang, W. G. Wallace-Freedman, S.-W. Chen, P. G. Schultz, *Science* **1995**, *268*, 1738–1740; b) E. Danielson, J. H. Golden, E. W. McFarland, C. M. Reaves, W. H. Weineberg, X. D. Wu, *Nature* **1997**, *389*, 944–948.
- [6] a) F. M. Menger, A. V. Eliseev, V. A. Migulin, *J. Org. Chem.* **1995**, *60*, 6666–6667; b) P. C. Michels, Y. L. Khmelitsky, J. S. Dordick, D. S. Clark, *Trends Biotechnol.* **1998**, *16*, 210–216.
- [7] S. Brocchini, K. James, V. Tangpasuthadol, J. Kohn, *J. Am. Chem. Soc.* **1997**, *119*, 4553–4554.
- [8] P. Timmerman, D. N. Reinhoudt, *Adv. Mater.* **1999**, *11*, 71–74.
- [9] a) I. Huc, J.-M. Lehn, *Proc. Natl. Acad. Sci. USA* **1997**, *94*, 2106–2110; b) F. M. Menger, A. V. Peresypkin, *J. Am. Chem. Soc.* **2001**, *123*, 5614–5615.
- [10] a) T. Shimizu, M. Kogiso, M. Masuda, *Nature* **1996**, *383*, 487–488; b) T. Shimizu, M. Masuda, *J. Am. Chem. Soc.* **1997**, *119*, 2812–2818;

- c) M. Kogiso, S. Ohnishi, K. Yase, M. Masuda, T. Shimizu, *Langmuir* **1998**, *14*, 4978–4986; d) T. Shimizu, R. Iwaura, M. Masuda, T. Hanada, K. Yase, *J. Am. Chem. Soc.* **2001**, *123*, 5947–5955; e) I. Nakazawa, M. Masuda, Y. Okada, T. Hanada, K. Yase, M. Asai, T. Shimizu, *Langmuir* **1999**, *15*, 4757–4764; f) M. Masuda, T. Hanada, K. Yase, T. Shimizu, *Macromolecules* **2000**, *33*, 9233–9238.
- [11] G. John, M. Masuda, Y. Okada, K. Yase, T. Shimizu, *Adv. Mater.* **2001**, *13*, 715–718.
- [12] J. H. P. Tyman, *Chem. Soc. Rev.* **1979**, *8*, 499–537.
- [13] a) A. S. Goldstein, A. N. Lukyanov, P. A. Carlson, P. Yager, M. H. Gelb, *Chem. Phys. Lipids*, **1997**, *88*, 21–36; b) D. D. Archibald, S. Mann, *Chem. Phys. Lipids*, **1994**, *69*, 51–64; c) J.-H. Fuhrhop, C. Boettcher, *J. Am. Chem. Soc.* **1990**, *112*, 1768–1776.
- [14] a) M. S. Spector, J. V. Selinger, A. Singh, J. M. Rodriguez, R. R. Price, J. M. Schnur, *Langmuir* **1998**, *14*, 3493–3500; b) B. N. Thomas, C. R. Safinya, R. J. Plano, N. A. Clark, *Science* **1995**, *267*, 1635–1638; c) M. S. Spector, A. Singh, P. B. Messersmith, J. M. Schnur, *Nano Lett.* **2001**, *7*, 375–378.
- [15] CD measurements for the mixtures of **1** and **2** were conducted especially at concentrations at which the binary mixtures form helical ribbons or nanotubes on self-assembly in water (e.g. 80% monoene and 20% saturated). However the mixtures showed similar CD signals to the pure monoene.
- [16] J. V. Selinger, M. S. Spector, J. M. Schnur, *J. Phys. Chem. B* **2001**, *105*, 7157–7169.

Received: May 28, 2002 [F4126]